Cofactor molecules maintain infectious conformation and restrict strain properties in purified prions

Nathan R. Deleault[a], Daniel J. Walsh[a], Justin R. Piro[a], Fei Wang[b], Xinhe Wang[b], Jiyan Ma[b], Judy R. Rees[c], and Surachai Supattapone[a,d,1]

Departments of [a]Biochemistry, [c]Community and Family Medicine (Biostatistics and Epidemiology), and [d]Medicine, Dartmouth Medical School, Hanover, NH 03755; and [b]Department of Molecular and Cellular Biochemistry, Ohio State University School of Medicine, Columbus, OH 43210

Edited* by Reed B. Wickner, National Institutes of Health, Bethesda, MD, and approved May 30, 2012 (received for review April 27, 2012)

Prions containing misfolded prion protein (PrP^{Sc}) can be formed with cofactor molecules using the technique of serial protein misfolding cyclic amplification. However, it remains unknown whether cofactors materially participate in maintaining prion conformation and infectious properties. Here we show that withdrawal of cofactor molecules during serial propagation of purified recombinant prions caused adaptation of PrP^{Sc} structure accompanied by a reduction in specific infectivity of $>10^5$-fold, to undetectable levels, despite the ability of adapted "protein-only" PrP^{Sc} molecules to self-propagate in vitro. We also report that changing only the cofactor component of a minimal reaction substrate mixture during serial propagation induced major changes in the strain properties of an infectious recombinant prion. Moreover, propagation with only one functional cofactor (phosphatidylethanolamine) induced the conversion of three distinct strains into a single strain with unique infectious properties and PrP^{Sc} structure. Taken together, these results indicate that cofactor molecules can regulate the defining features of mammalian prions: PrP^{Sc} conformation, infectivity, and strain properties. These findings suggest that cofactor molecules likely are integral components of infectious prions.

phospholipid | bioassay | repertoire | convergence | diversity

Transmissible spongiform encephalopathies such as Creutzfeldt–Jakob disease, bovine spongiform encephalopathy, chronic wasting disease, and scrapie are caused by unconventional infectious agents termed "prions" that lack informational nucleic acids (1). The most fundamental event in the formation of infectious prions is the conformational change of a host-encoded glycoprotein termed "PrP^{C}" into a misfolded conformer termed "PrP^{Sc}" (2, 3); purified PrP^{Sc} molecules can induce the conversion of additional PrP^{C} molecules into the PrP^{Sc} conformer in a self-propagating manner (4, 5).

Much effort has been made to determine the chemical nature of infectious mammalian prions. According to the "protein-only" hypothesis, infectious prions potentially are composed solely of PrP^{Sc} (6–9). However, several groups have shown that relatively low levels of specific infectivity using only pure PrP molecules as a substrate (10–12). In contrast, chemical reactions containing purified PrP molecules plus nucleic acid and lipid molecules spontaneously generate and propagate PrP^{Sc} molecules associated with moderate levels of specific infectivity (5). Additional evidence that cellular factors other than PrP influence the efficiency of prion propagation is provided by studies showing that various clonal lines of cultured neuroblastoma cells have different levels of susceptibility to prion infection (13, 14). It is unknown currently whether cofactor molecules are simply catalysts for prion formation or whether they also play an essential role maintaining a specific infectious conformation of PrP^{Sc}. Studies with purified prions containing a photolabile oligonucleotide cofactor showed that polyanionic cofactors are not required to maintain infectivity (15), but the prions used in those studies contained copurified lipids, whose role in maintaining infectivity remains unknown.

Interestingly, prions can exist as different "strains" characterized by distinctive clinical and neuropathological features that are recapitulated faithfully upon serial passage within the same animal species (16, 17). Recent studies suggest that individual strains of mammalian prions may be composed of a mixture of PrP^{Sc} conformers and that the relative distribution of those conformers may be subject to selective pressure during the process of strain adaptation, e. g., by transmission between different animal species (18) or passage in cloned cell lines (19). However, the molecular mechanism by which a variety of PrP^{Sc} conformers can be produced and selected during the process of strain adaptation has not yet been elucidated. One possible mechanism is that each PrP^{Sc} conformer might require a unique set of cofactors to propagate efficiently, and the distribution of these putative cofactor molecules may vary in different animal species and cell types. Consistent with this concept, reconstitution studies have revealed the existence of multiple classes of cofactors for prion propagation in vitro (20).

We recently identified the endogenous activity responsible for facilitating mouse prion propagation in vitro (20) as phosphatidylethanolamine (PE) (21). PE robustly facilitates the formation of infectious recombinant mouse prions as a solitary cofactor without RNA, providing a unique tool to test whether cofactor molecules can regulate PrP^{Sc} conformation, prion strain properties, and infectivity in a minimal in vitro prion propagation system.

Results

Withdrawal of Cofactor During Serial Propagation Produces an Adapted Self-Propagating "Protein-only" PrP^{Sc} Conformer. We serially propagated a previously described recombinant prion strain (22) (termed the "OSU strain") for more than 30 rounds in seeded serial protein misfolding cyclic amplification (sPMCA) reactions using a substrate mixture containing pure α-helical recombinant prion protein (recPrP) molecules and a purified cofactor preparation containing a mixture of mouse brain phospholipids, of which the only active component is PE. Under these conditions, the propagation of an ~18-kDa PrP^{Sc} conformer (which we term "OSU cofactor PrP^{Sc}") is maintained indefinitely (Fig. 1*A*, first blot). To test whether cofactor molecules are required to maintain a self-propagating PrP^{Sc} conformation, we used OSU cofactor PrP^{Sc} molecules to seed sPMCA reactions with recPrP as the sole substrate (i.e., without the cofactor preparation). These experiments produced two different

Author contributions: N.R.D. and S.S. designed research; N.R.D., D.J.W., J.R.P., and S.S. performed research; N.R.D., J.R.P., F.W., X.W., and S.S. contributed new reagents/analytic tools; N.R.D., J.R.R., and S.S. analyzed data; and N.R.D., D.J.W., J.M., J.R.R., and S.S. wrote the paper.

Conflict of interest statement: S.S. and N.D. are inventors on a patent held by Dartmouth College on the use of phosphatidylethanolamine as a prion cofactor.

*This Direct Submission article had a prearranged editor.

[1]To whom correspondence should be addressed. E-mail: supattapone@dartmouth.edu.

See Author Summary on page 11074 (volume 109, number 28).

This article contains supporting information online at www.pnas.org/lookup/suppl/doi:10.1073/pnas.1206999109/-/DCSupplemental.

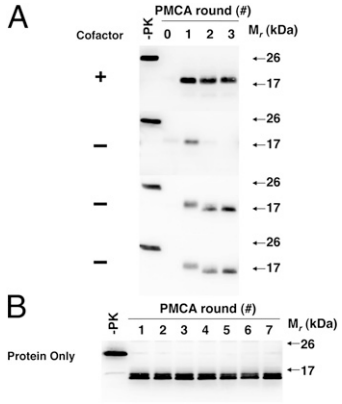

Fig. 1. Adaptation of autocatalytic PrP^{Sc} molecules. Western blots of reconstituted sPMCA reactions. –PK, samples not subjected to proteinase K digestion; all other samples were proteolyzed. (*A*) All reactions initially were seeded with OSU cofactor PrP^{Sc} molecules and subsequently were propagated in substrate mixtures with or without cofactor, as indicated. (*B*) Ongoing propagation of OSU protein-only PrP^{Sc} molecules in substrate mixture lacking cofactor.

sets of outcomes. In ~40% of these experiments, PrP^{Sc} propagation could not be sustained following cofactor withdrawal (Fig. 1*A*, second blot), but in ~60% of the experiments we unexpectedly observed step-wise adaptation of the ~18-kDa OSU cofactor PrP^{Sc} seed into a self-propagating ~16-kDa protease-resistant recPrP^{Sc} band (which we term "OSU protein-only PrP^{Sc}") (Fig. 1*A*, third and fourth blots). The resistance of the OSU protein-only PrP^{Sc} conformer to digestion with a 25:1 mass ratio of proteinase K to recPrP, as well as its formation in the absence of 0.1% SDS, distinguishes it from a previously reported recPrP sPMCA product (23). Once formed, the OSU protein-only PrP^{Sc} conformer could be propagated indefinitely in sPMCA reactions (Fig. 1*B*) in the same manner as the cofactor PrP^{Sc} conformer. Interestingly, the OSU protein-only PrP^{Sc} conformer did not trigger formation of ~18-kDa recPrP^{Sc} when either the purified cofactor preparation or synthetic PE was restored to the substrate mixture (Fig. S1), indicating that the switch from the cofactor PrP^{Sc} conformation to the protein-only PrP^{Sc} conformation is unidirectional.

Cofactor PrP^{Sc} and Protein-only PrP^{Sc} Molecules Have Similar Ultrastructural Features. To compare the ultrastructural characteristics of the OSU cofactor PrP^{Sc} conformer with those of the OSU protein-only PrP^{Sc} conformer, we performed atomic force microscopy on both types of PrP^{Sc} molecules. This comparison revealed that the two conformers generally displayed similar ultrastructural features (the predominant species observed in both samples being an ~2-nm sphere), although the distribution of heights differed slightly between the two samples (Fig. S2 *A* and *B*). Rings ~100 nm in diameter also were seen in ~1% of the scanned fields in the sample containing protein-only PrP^{Sc} molecules (Fig. S2*A*, *Right*). Interestingly, these recPrP^{Sc} spheres and rings are reminiscent of previously described "dots and rings" formed by yeast prions (24, 25). No fibrils were observed in scans of either OSU cofactor PrP^{Sc} or OSU protein-only PrP^{Sc} molecules.

Protein-only PrP^{Sc} Molecules Are Not Infectious in Vivo and Cannot Trigger Native PrP^{Sc} Formation in Vitro. We next sought to compare the infectivity of OSU cofactor PrP^{Sc} and OSU protein-only PrP^{Sc} molecules. To do so rigorously, we generated a closely matched set of internally controlled samples. Substrate mixtures were prepared from two aliquots of a single stock solution of recPrP in buffer. Then purified cofactor was added to one of the aliquots to complete the cofactor PrP^{Sc} mixture, and an equal volume of water was added to the other aliquot to make the protein-only mixture. We then simultaneously propagated OSU cofactor PrP^{Sc} and OSU protein-only PrP^{Sc} molecules in their appropriate substrate mixtures using equidistant, concentric locations of a single circular microplate horn. SDS/PAGE of the final round products shows that similar quantities of PrP^{Sc} were produced in all the processed samples (Fig. S3). Thus, the availability of these well-matched and simultaneously processed samples provided a unique opportunity to test in isolation the role of cofactor molecules in maintaining prion infectivity.

We performed end-point titration bioassays of these simultaneously processed samples in wild-type C57BL mice. The results of these assays indicate that recPrP^{Sc} molecules formed with cofactor caused scrapie at dilutions from 10^{-1} to 10^{-5} (Table 1), as confirmed by pathology (Fig. S4) and Western blot (Fig. S5). Based on the end-point titration data and Western blot quantitation of PrP^{Sc} in the inoculum, the specific infectivity of OSU cofactor recPrP^{Sc} molecules is $\sim 2.2 \times 10^6$ LD_{50} units/μg PrP. In contrast, OSU protein-only recPrP^{Sc} molecules derived from the same original recPrP^{Sc} seed failed to cause scrapie in mice even at the highest concentration tested (Table 1). The brains of age-matched, asymptomatic animals inoculated with protein-only recPrP^{Sc} molecules were histologically normal (Fig. S4) and lacked PrP^{Sc} as judged by Western blot (Fig. S5).

To determine whether the $>10^5$-fold difference in specific infectivity is caused by differences in the ability of the two PrP^{Sc} conformers to trigger native PrP^{C} conversion, we compared the ability to these two conformers to seed sPMCA reactions using crude brain homogenate as substrate. The results show that although the OSU cofactor PrP^{Sc} molecules effectively seeded PrP^{Sc} formation, the OSU protein-only PrP^{Sc} conformer failed to trigger native prion formation in all three rounds of the sPMCA assay (Fig. 2). Moreover, the inability of the OSU protein-only conformer to trigger native PrP^{C} conversion could not be overcome by preliminary propagation for four rounds in a substrate mixture containing PE before sPMCA with brain homogenate (Fig. S6), confirming that the switch to the inactive conformation is most likely irreversible and that phospholipid molecules do not simply protect or enhance delivery of PrP^{Sc}. Collectively, the results of the bioassay and sPMCA experiments show that controlled removal of cofactor causes adaptation of self-propagating, protease-resistant recPrP^{Sc} molecules into a conformation that is unable to trigger native PrP^{Sc} formation in vivo or in vitro.

Cofactor Molecules Are Physically Associated with PrP^{Sc} Aggregates. Because the foregoing results indicate that a cofactor prepara-

Table 1. Bioassay of in vitro-generated recombinant PrP^{Sc} molecules in normal C57BL mice

Inoculum	Dilution	n/n_0	IP (days)*
Cofactor PrP^{Sc}	10^{-1}	7/7	356 ± 12
	10^{-2}	3/3	451 ± 16
	10^{-3}	4/4	481 ± 42
	10^{-4}	4/4	501 ± 28
	10^{-5}	1/3	539
	10^{-6}	0/4	>570
Protein only PrP^{Sc} Sample A	10^{-1}	0/4	>570
	10^{-2}	0/4	>570
	10^{-3}	0/4	>570
	10^{-4}	0/4	>570
Protein only PrP^{Sc} Sample B	10^{-1}	0/4	>570
	10^{-2}	0/4	>570
	10^{-3}	0/4	>570
	10^{-4}	0/4	>570

*Incubation period (IP) of scrapie sick animals, mean ± SE.

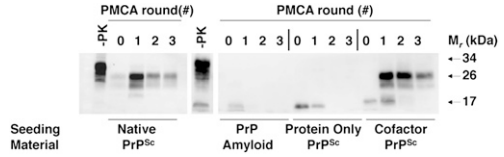

Fig. 2. Seeding of brain homogenate sPMCA reactions. Western blot of three-round sPMCA reactions using normal mouse brain homogenate substrate seeded with various samples as indicated. −PK, samples not subjected to proteinase K digestion; all other samples were proteolyzed. Native PrP^{Sc} was isolated as PrP27-30 molecules from the brains of Me7-infected mice as previously described (35), and PrP amyloid was generated as previously described (36).

tion containing PE is required to maintain PrP^{Sc} infectivity, we sought to determine whether PE becomes physically incorporated into the recombinant prion aggregates as they are formed. To study this question, we used the compound 1-oleoyl-2-{12-[(7-nitro-2–1,3-benzoxadiazol-4-yl)amino]dodecanoyl}-sn-glycero-3-phosphoethanolamine [18:1–12:0 nitrobenzoxadiazole (NBD):PE], in which a fluorescent NBD group is covalently attached as a probe to the C_2 fatty acid adduct of synthetic PE. We performed seeded four-round sPMCA reactions with a substrate mixture containing recPrP and NBD-PE to produce NBD-PE PrP^{Sc} molecules (Fig. 3*A*). We then used a microscopic dual-channel fluorescence assay to determine whether NBD-PE became incorporated into complexes with $recPrP^{Sc}$ during the sPMCA reactions. The results of this assay show that the fluorescent cofactor is present and colocalizes with PrP^{Sc} aggregates detected by antibody staining (Fig. 3*B*), indicating that the recombinant prions do contain PE in addition to PrP^{Sc} molecules. Quantitation of total NBD fluorescence within the washed $recPrP^{Sc}$ pellet suggests a protein:lipid molar ratio of ∼1:4. It is unlikely that the fluorescent lipid molecules are weakly bound to the solvent-accessible surface of PrP^{Sc} aggregates because the samples were washed extensively with detergent before analysis.

Cofactor-Induced Modulation of Strain-Dependent Neurotropism and Prion Incubation Times. The observation that cofactor molecules participate in maintaining the infectious conformation of PrP^{Sc} raises the possibility that they also may play a role in encoding strain properties. Castilla et al. (26) previously established that several different murine prion strains maintain their specific biochemical and infectious properties when serially propagated

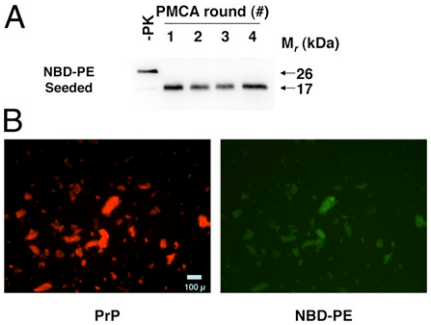

Fig. 3. NBD-PE PrP^{Sc} colocalization assay. (*A*) Western blot of a four-round sPMCA reaction using recPrP and NBD-PE as substrate. −PK, samples not subjected to proteinase K digestion; all other samples were proteolyzed. (*B*) Dual-channel fluorescence micrographs showing representative images of the final product of the sPMCA reaction shown in *A*, after purification with detergent washes as described in *Experimental Procedures*. PrP^{Sc} aggregates immunostained with anti-PrP mAb D13 and Alexa Fluor 568-labeled secondary antibody are shown in red (PrP), and colocalized NBD-PE molecules are shown in green (NBD-PE).

in vitro using crude brain homogenate as a substrate. Therefore, we decided to use our chemically defined in vitro prion propagation system to test whether different prion strains are able to maintain distinctive properties when only one active cofactor (PE) is available to form new PrP^{Sc} molecules.

For these experiments, we used the original OSU isolate [which was produced de novo in sPMCA reactions from recPrP, 1-palmitoyl-2-oleoyl-sn-glycero-3-phosphoglycerol (POPG), and RNA substrates (22)] as well as two easily distinguishable native mouse prion strains (301C and Me7) to seed a uniform substrate mixture containing recPrP and purified cofactor preparation. For each strain, sPMCA produced self-propagating cofactor $recPrP^{Sc}$ molecules with a protease-resistant core ∼18 kDa in size (Fig. S7*A*).

We inoculated wild-type C57BL mice with cofactor PrP^{Sc} molecules produced by 18-round sPMCA propagation of each strain along with the original seed material (input samples) for each strain and negative control samples. Mock-propagated samples originally seeded with each strain and processed in parallel with the experimental samples were noninfectious, confirming that 18 rounds of sPMCA were sufficient to eliminate the original infectious seeds by serial dilution (Table 2). In contrast, cofactor PrP^{Sc} molecules derived from all three strains caused scrapie in the inoculated animals. Interestingly, the incubation periods for cofactor PrP^{Sc} molecules were at least twice as long as the incubation periods caused by the input samples for all three strains (Table 2).

The defining characteristic of mammalian prion strains is selective neurotropism in infected hosts, and therefore we analyzed the neuropathological profiles of mice inoculated with input and cofactor PrP^{Sc} molecules by scoring brain regions for spongiform change (vacuolation) and PrP deposition (immunohistochemistry). As expected, the three input strains could be distinguished from each other easily by their vacuolation and PrP deposition profiles (Fig. 4 *A* and *E*). However, the vacuolation and PrP deposition profiles for all three cofactor PrP^{Sc} samples derived from those strains were similar to each other (Fig. 4 *B* and *F*) and were different from their parent strains (i.e., the three input samples) (compare vacuolation profiles in Fig. 4 *A* and *B* and PrP deposition profiles in Fig. 4 *E* and *F*).

At a microscopic level, the most dramatic examples of cofactor-induced changes in neurotropism that we observed were in (*i*) the degree of vacuolation caused by OSU input versus OSU cofactor PrP^{Sc} molecules in the cerebral cortex and hypothalamus (Fig. S8) and (*ii*) the patterns of PrP immunodeposition induced by 301C input versus 301C cofactor PrP^{Sc} molecules in the cerebral cortex (where 301C input causes deposition selectively in cortical layers III–IV, as indicated by the arrowhead in Fig. S9).

It is important to note that both the OSU input and OSU cofactor PrP^{Sc} samples were produced by propagation of the original OSU seed (containing POPG and RNA) in sPMCA reactions using recPrP substrate. The only experimental difference between these two samples was a change in the cofactor component from POPG/RNA to the purified phospholipid cofactor preparation of the sPMCA substrate mixture. Therefore, in this case, the dramatic differences in neurotropism between the OSU input and OSU cofactor PrP^{Sc} samples (Fig. 4, red squares; compare Fig. 4 *A* and *B* with *F* and *E*) can be attributed unambiguously to the change in cofactor composition and not to the use of recPrP substrate or to the sPMCA technique per se in the experiment.

Because the only component of the purified cofactor preparation able to facilitate PrP^{Sc} propagation is PE, we hypothesized that PE alone might be responsible for producing and maintaining the characteristics of the cofactor PrP^{Sc} strain, which differ markedly from those of each of the three input strains. To test this hypothesis, we propagated all three sets of cofactor PrP^{Sc} molecules into a substrate mixture containing only recPrP and synthetic PE for 18 rounds, yielding a set of "PE PrP^{Sc}"

Table 2. Bioassay of native and in vitro-generated recombinant PrP^{Sc} molecules in normal C57BL mice

Seed (strain)	Inoculum	Dilution	n/n_0	IP (days)*
OSU	Input $recPrP^{Sc}$	10^0	5/5	173 ± 1
OSU	Cofactor $recPrP^{Sc}$	10^{-1}	7/7	356 ± 12
OSU	Synthetic PE $recPrP^{Sc}$	10^{-1}	8/8	381 ± 11
OSU	Serial Passage- Synthetic PE $recPrP^{Sc}$	1% wt/vol	8/8	175 ± 4
OSU	Mock sPMCA control	10^{-1}	0/4	>570
Me7	Input brain homogenate	10^{-1}	7/7	158 ± 7
Me7	Cofactor $recPrP^{Sc}$	10^{-1}	8/8	396 ± 20
Me7	Synthetic PE $recPrP^{Sc}$	10^{-1}	6/6	417 ± 21
Me7	Serial Passage- Synthetic PE $recPrP^{Sc}$	1% wt/vol	8/8	166 ± 3
Me7	Mock sPMCA control	10^{-1}	0/4	>510
301C	Input brain homogenate	10^{-1}	7/7	182 ± 4
301C	Cofactor $recPrP^{Sc}$	10^{-1}	8/8	401 ± 11
301C	Synthetic PE $recPrP^{Sc}$	10^{-1}	6/7	360 ± 9†
301C	Serial Passage- Synthetic PE $recPrP^{Sc}$	1% wt/vol	8/8	173 ± 3
301C	Mock sPMCA control	10^{-1}	0/4	>510
None	Cofactor mixture	10^{-1}	0/4	>570
None	Synthetic PE mixture	10^{-1}	0/4	>570

*Incubation period (IP) of scrapie sick animals, mean ± SE.
†Ongoing experiment. n/n_0 = number of animals diagnosed with prion disease/number of animals inoculated.

molecules also ~18 kDa in size (Fig. S7*B*). When inoculated into C57BL mice, all three sets of PE PrP^{Sc} molecules caused scrapie with long incubation periods comparable to those induced by cofactor PrP^{Sc} molecules (Table 2). Neuropathological studies showed that all three sets of PE PrP^{Sc} inocula induced similar patterns of vacuolation and PrP deposition in the brains of inoculated mice (Fig. 4 *C* and *G*). Moreover, these patterns were similar to those induced by cofactor PrP^{Sc} molecules (compare vacuolation profiles in Fig. 4 *C* and *B* and PrP deposition profiles in Fig. 4 *F* and *G*).

Statistical analysis confirmed that vacuolation patterns of the three cofactor PrP^{Sc} samples were significantly different (Wilcoxon rank-sum test $P < 0.05$) from their corresponding three input strains in 18 of 21 comparisons (seven brain regions and three output inocula). Similarly, PrP immunodeposition of OSU input- versus OSU cofactor PrP^{Sc}-inoculated animals showed statistically significant differences in seven of eight brain regions, Me7 input- versus Me7 cofactor PrP^{Sc}-inoculated animals showed statistically significant differences in two of eight brain regions, and 301C input- versus 301C cofactor PrP^{Sc}-inoculated animals showed statistically significant differences in five of eight brain regions. Additional statistical analysis showed no evidence to reject the hypothesis that the vacuolation and PrP deposition profiles of the six output (cofactor and PE) strains came from a single distribution. In contrast, when the analysis was repeated after including the three input strains and six output strains, the null hypothesis was rejected for six of the eight brain regions (all $P < 0.04$).

Cofactor-Induced Modulation of Strain-Dependent PrP^{Sc} Conformation. In some instances, differences in the conformation of PrP^{Sc} molecules associated with different prion strains can be detected by biochemical assays. We therefore compared biochemical characteristics of PrP^{Sc} molecules in the brains of infected mice by SDS/PAGE/Western blotting and urea denaturation assays. Western blotting showed that all three sets of cofactor PrP^{Sc} inocula induced the formation of protease-resistant PrP^{Sc} molecules with similar glycoform profiles (dominated by diglycosylated PrP^{Sc}) and migration after enzymatic deglycosylation (Fig. 5, lanes 1–3). Similarly, the protease-resistant PrP^{Sc} molecules in the brains of animals infected with all three sets of PE PrP^{Sc} inocula had glycoform profiles and migration patterns that were similar to those of PrP^{Sc} molecules in the brains of animals infected with cofactor PrP^{Sc} inocula (Fig. 5, compare lanes 7–9 with lanes 1–3). In contrast, protease-resistant PrP^{Sc} molecules induced by input 301C prions were ~2 kDa smaller in size (Fig. 5, lane 4), and PrP^{Sc} molecules induced by input OSU recombinant prions had a characteristic glycoform profile in which diglycosylated PrP^{Sc} was the least abundant species (Fig. 5, lane 6).

We used a urea denaturation assay to compare PrP^{Sc} stability in the brains of mice infected with the various sets of inocula. The results revealed significant differences in the conformational stability of PrP^{Sc} molecules in the brains of animals inoculated with the three input strains (Fig. 6*A*). PrP^{Sc} molecules induced by the OSU input strain were the most resistant to urea denaturation [$(Urea)_{1/2}$ = 3.8 M], whereas input Me7-induced PrP^{Sc} molecules were the most susceptible to denaturation, with [$(Urea)_{1/2}$ = 2.0 M]. In contrast, the PrP^{Sc} molecules in the brains of mice inoculated with the three sets of cofactor PrP^{Sc} molecules (Fig. 6*B*) as well as the three sets of PE PrP^{Sc} inocula (Fig. 6*C*) all displayed similar denaturation profiles [$(Urea)_{1/2}$ = 1.5–2.2 M]. It is interesting that the relatively weak resistance to denaturation exhibited by PrP^{Sc} molecules in cofactor PrP^{Sc}- and PE PrP^{Sc}-inoculated mice was unexpected, given their long scrapie incubation times (Table 2), because it had been suggested previously that long incubation times in mice usually are correlated with a high level of PrP^{Sc} conformational stability (27).

Strain Adaptation upon Serial Passage in Vivo. Finally, we investigated whether the unique strain properties of cofactor PrP^{Sc} and PE PrP^{Sc} molecules would be maintained upon serial passage in mice. The results of these analyses showed that all six sets of serially passaged prions (i.e., the brains of cofactor PrP^{Sc}- and PE PrP^{Sc}-inoculated animals for all three strains) displayed incubation times (Table 2), patterns of neurotropism (Fig. 4 *D* and *H*), and PrP^{Sc} biochemical characteristics (Fig. 6 and Fig. S10) that were similar to each other. These results confirm that all the cofactor PrP^{Sc} and PE PrP^{Sc} prions had converged into a single strain. The biochemical characteristics of the PrP^{Sc} molecules in the brains of animals inoculated with each of the serially passaged prions also were indistinguishable from those of the PrP^{Sc} molecules in the brains of animals directly inoculated with cofactor PrP^{Sc} and PE PrP^{Sc} prions (Fig. 6 and Fig. S10). However, the

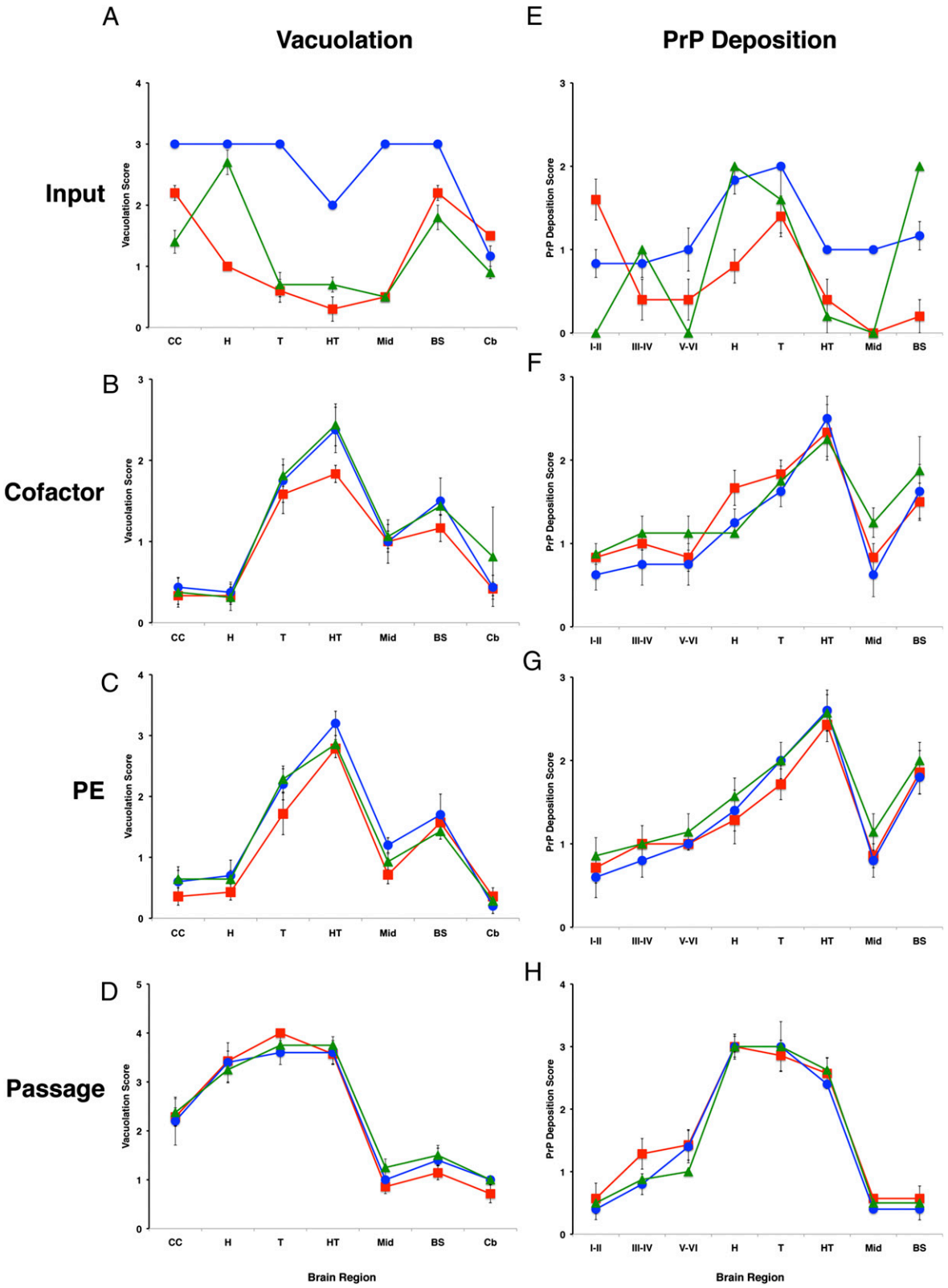

Fig. 4. Regional neuropathology of infected mice. (*A–D*) Profiles of vacuolation scores of animals inoculated with samples containing (*A*) input prions, (*B*) cofactor PrP^{Sc} molecules, (*C*) PE PrP^{Sc} prions, or (*D*) serial-passage PE PrP^{Sc} prions. (*E–H*) Profiles of PrP deposition scores of animals inoculated with samples containing (*E*) input prions, (*F*) cofactor PrP^{Sc} molecules, (*G*) PE PrP^{Sc} prions, or (*H*) serial-passage PE PrP^{Sc} prions. Prion strains: OSU, red squares; Me7, blue circles; 301C, green triangles. Brain regions: I–II, cerebral cortical layers 1 and 2; III–IV, cortical layers 3 and 4; V–VI, cortical layers 5 and 6; BS, brainstem; Cb, cerebellum; CC, cerebral cortex (all layers); H, hippocampus; HT, hypothalamus; Mid, midbrain; T, thalamus. Mean values ± SEM are shown; $n = 5$.

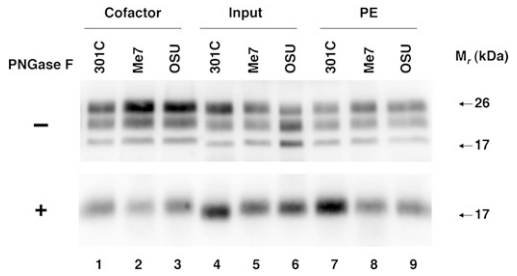

Fig. 5. Glycoform distribution and electrophoretic mobility of PrP^{Sc} molecules in the brains of infected mice. (*Upper*) Western blots of brain homogenate samples prepared from animals inoculated with samples containing input prions, cofactor PrP^{Sc}, and PE PrP^{Sc} molecules derived from different prion strains, as indicated. All samples were subjected to limited proteolysis. (*Lower*) Samples also were deglycosylated by treatment with PNGase F, as indicated (+), before SDS/PAGE.

prion incubation times and patterns of neurotropism of the second-passage prions differed from those of the cofactor PrP^{Sc} and PE PrP^{Sc} prions (Table 2 and Fig. 4; compare vacuolation profiles in Fig. 4 *C* and *D* and PrP deposition profiles in Fig. 4 *G* and *H*), indicating that additional strain adaptation occurred during in vivo propagation, presumably because of the availability of additional cellular cofactors in the intact brain.

Discussion

In this paper we used a minimal in vitro prion propagation system to study directly the effect of cofactor molecules on PrP^{Sc} conformation, infectivity, and strain properties. Our results show that withdrawal of cofactor during serial propagation of purified recombinant prions caused adaptation of PrP^{Sc} conformation, manifest as an ~2-kDa difference in the size of the protease-resistant core. Moreover, a direct comparison between samples of cofactor-containing and protein-only PrP^{Sc} molecules (produced in parallel from the same seed and substrate mixture) using an end-point titration bioassay revealed that phospholipid molecules play a quantitatively large role in maintaining the infectivity of in vitro-generated prions. In contrast, RNA molecules are not required to maintain infectivity in the presence of copurified lipids and therefore can be considered nonessential (15). Our results may help explain why relatively modest levels of infectivity are produced when purified recPrP (presumably containing little or no bacterial lipid) has been used as a solitary substrate to generate prions by a variety of protocols (10–12, 28). Although we cannot rule out the possibility that a yet unidentified protocol could produce highly infectious prions from recPrP alone, the results of our internally controlled experiment in which an alternative, noninfectious PrP^{Sc} conformation is propagated after cofactor withdrawal suggest that this scenario is not likely to occur and that the infectious conformation of PrP^{Sc} is structurally dependent on physical interactions between PrP and essential cofactor molecules.

We also found that cofactor molecules seem to exert an influence on prion strain properties in our minimal prion propagation system. Most importantly, we found that the strain properties of recombinant prions initially formed from recPrP substrate by sPMCA with POPG and RNA molecules could be altered during subsequent serial propagation by changing only the cofactor component (from POPG/RNA to PE) to form a unique output strain characterized by a long scrapie incubation period and unique neuropathological and biochemical characteristics. These results directly show that a change in cofactor, rather than the absence of cellular processes, is sufficient to cause a change in prion strain properties. Additional experiments revealed that that two different native prion strains also adapted into the same unique output strain when propagated in vitro with PE as the only available cofactor. Given the clear differences among three input prion strains, our results indicate that a single cofactor can selectively pressure multiple prion strains to converge into a single, phenotypically distinct strain.

Prior studies have shown that strain properties are not altered either randomly or as a result of cross-contamination in seeded sPMCA reactions (26, 29). These potential pitfalls also are very unlikely to explain the results of our experiments because (*i*) a completely unique strain was produced reproducibly in all six independent samples containing PE; (*ii*) each sample was propagated in its own sonicator horn; (*iii*) each sample was propagated at a different time; (*iv*) the reaction tubes were sealed with Parafilm, a maneuver that eliminates cross-contamination during sPMCA (30); and (*v*) the OSU input and OSU cofactor PrP^{Sc} samples exhibit different strain characteristics, but both samples are products of sPMCA reactions with recPrP substrate seeded with OSU prions.

It is interesting to speculate that individual prion strains may propagate most efficiently with their own unique set of endogenous cellular cofactors and that the levels of these particular cofactors may vary among cell types and animal species. Various types and combinations of cofactors easily could account for the natural diversity of prion strains. This "cofactor selection" hypothesis provides a potential molecular mechanism for the generation of multiple PrP^{Sc} conformations (31) (potentially because of the interaction of PrP with multiple potential cofactors) that can adapt in response to selective pressure in cell cultures (19) or cross-species transmission (18) as well as for the phenomenon of strain-specific neurotropism (if strain-specific cofactors are enriched selectively in different brain regions). This hypothesis also is consistent with the generation of unique strain phenotypes that have been reported when infectious prions are produced in the absence of endogenous cofactors (11, 12, 28). Cofactors capable of maintaining the properties of native murine prion strains in vitro are present in crude brain homogenate, because sPMCA in brain homogenate substrate has been shown to preserve the strain-specific characteristics of 301C and other murine prions (26, 29).

Taken together, our results show that cofactor molecules such as PE modulate PrP^{Sc} structure in infectious prions, enabling the formation of the infectious conformer and restricting strain properties. These findings suggest that cofactor molecules are likely integral and essential components of infectious prions. It is possible that cofactor molecules also may play a critical role in the pathogenesis of other neurodegenerative diseases in which protein misfolding can spread through the brain, such as Alzheimer's disease, Parkinson disease, and amyotrophic lateral sclerosis (32).

Experimental Procedures

Reagents. The Me7 (mouse adapted scrapie originally from sheep) and 301C (mouse adapted bovine spongiform encephalopathy prions) prion strains used in this study were kindly provided by Stanley Prusiner (University of California, San Francisco) and Claudio Soto (University of Texas, Houston), respectively. The recombinant strain designated "OSU" is the $recPrP^{Sc}$ sample originally produced de novo by F.W. as previously described (22) and subsequently propagated with purified cofactor by N.R.D. The pET-22b(+) expression plasmid (catalog no. 69744), Overnight Express Autoinduction System (catalog no. 71300–3), Bug Buster 10× plus Lyso catalog no. nase Kit (catalog no. 71370), and Ni-NTA His-Bind Superflow Resin (catalog no. 70691) were purchased from EMD Chemicals. Micrococcal (S7) nuclease (catalog no. 107921) was purchased from Roche. Thermolysin (catalog no. 88303) was purchased from Sigma. Synthetic plasmalogen phosphatidylethanolamine (PE) (catalog no. 852758P) was purchased from Avanti Polar Lipids.

Animal Care. Female C57BL mice were purchased from Charles River Laboratories (Wilmington, MA). Mice were housed in microisolation cages and handled in strict accordance with good animal practice, as defined by the Guide for the Care and Use of Laboratory Animals of the National Institutes of Health.

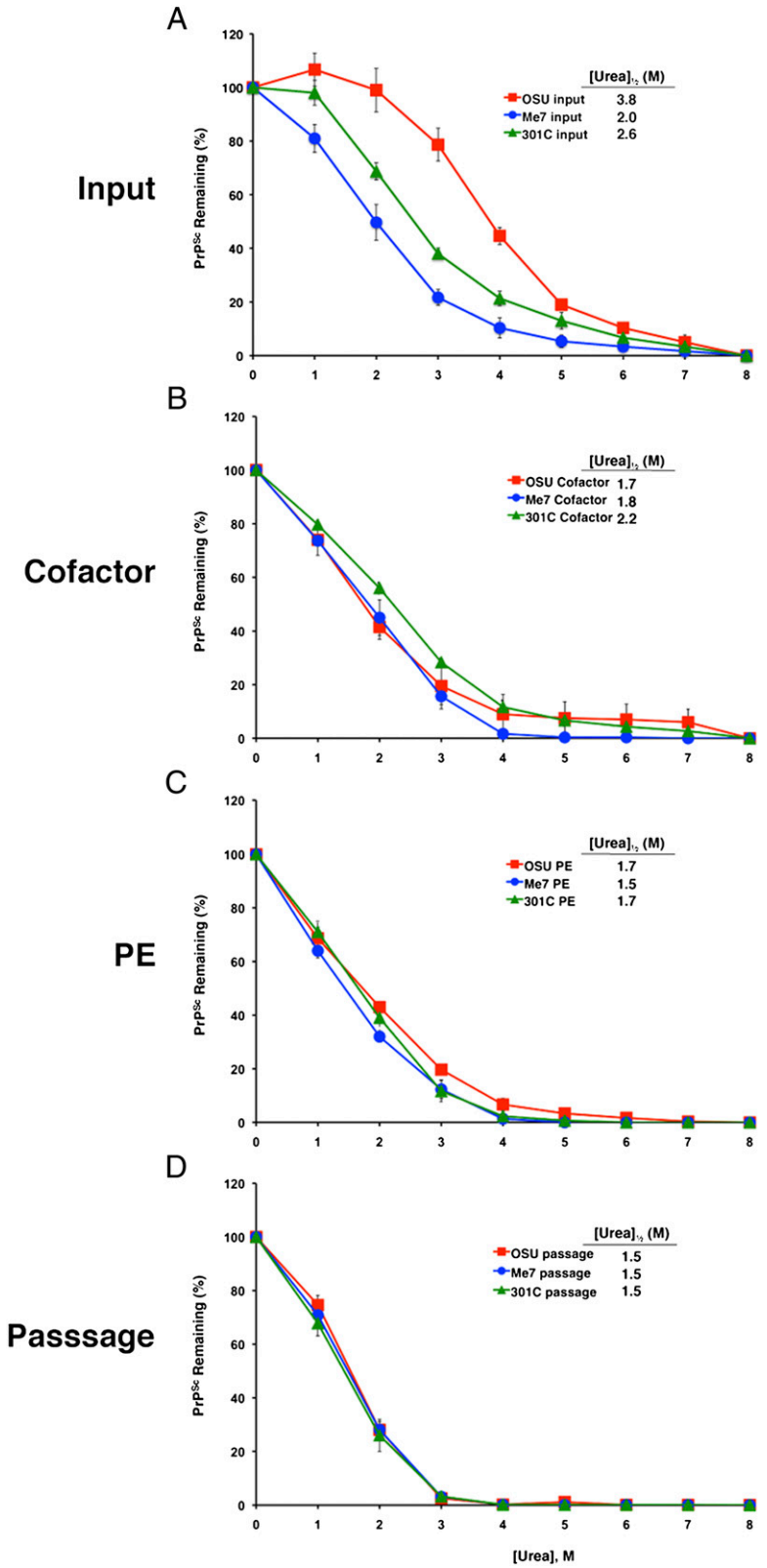

Fig. 6. Analysis of PrP^{Sc} conformational stability. Urea denaturation assay showing PrP^{Sc} levels in samples of brain homogenates prepared from animals inoculated with samples derived from different prion strains. Inocula were (*A*) input prions; (*B*) cofactor PrP^{Sc}; (*C*) PE PrP^{Sc}; (*D*) serial-passage PE PrP^{Sc}. OSU, red squares; Me7, blue circles; 301C, green triangles. Mean values ± SEM of three replicates are shown for each point.

The Dartmouth College Institutional Animal Care and Use Committee approved the animal work (assurance number A3259-01). Inoculations were performed under isoflurane anesthesia, and all efforts were made to minimize suffering.

Recombinant Mouse PrP Expression and Purification. Amplified DNA sequences coding for mouse PrP 23–231 were ligated into the pET-22b(+) expression vector (EMD Chemicals), and sequences were verified. The expression vector

then was transformed into *Escherichia coli* Rosetta Cells (EMD Chemicals). Cells were grown overnight in 1 L of LB medium (5 g yeast extract, 10 g Bacto tryptone, 10 g NaCl) supplemented with the Overnight Express Autoinduction System (EMD Chemicals). The next day the cells were centrifuged at 8,000 × *g* for 10 min, and the supernatant was discarded. Pellets were resuspended in a solution of 1× Bug Buster and 10 μL Lysonase (EMD Chemicals) containing EDTA-free Complete protease inhibitors (Roche). Cells then were incubated on ice and lysed using intermittent sonication for 20 min. The lysate was centrifuged at 16,000 × *g* for 20 min and was washed twice with 0.1× Bug Buster. The resulting inclusion bodies were solubilized using 8 M guanidine HCl and physical agitation, and insoluble material was removed by centrifugation at 8,000 × *g* for 15 min. PrP then was purified as described previously (22).

Cofactor Preparation. The protocol for isolating the cofactor preparation and details about its composition have been described previously (21). All centrifugation was done at 4 °C unless otherwise noted. A 10% (wt/vol) brain homogenate was made by processing 0.5 g normal mouse brain in 4.5 mL of 20 mM 3-(N-morpholino)propanesulfonic acid (Mops) (pH 7.0), 150 mM NaCl with a Potter homogenizer. Debris was removed by centrifugation at 200 × *g* for 30 s. The postnuclear supernatant was centrifuged for 30 min at 10,000 × *g*, and the resulting pellet was rehomogenized in 4.5 mL of 20 mM Mops (pH 7.0), 150 mM NaCl containing 3% (wt/vol) N-octyl-β-D-glucopyranoside (NOG) (Anatrace) and incubated at room temperature for 30 min. Next, the homogenate was centrifuged at 100,000 × *g* for 60 min. The resulting supernatant was adjusted to 2 mM $CaCl_2$ and 150 U/mL S7 nuclease (Roche) and was incubated at 37 °C for 30 min using an end-over-end rotator. Thermolysin (Sigma) was added at a final concentration of 25 μg /mL, and the sample was incubated at 70 °C for 60 min with intermittent mixing. Next, the sample was cooled on ice, adjusted to 5 mM EDTA, and centrifuged for 1 h at 100,000 × *g*. The supernatant then was placed in cellulose ester dialysis tubing with a 20,000 Molecular Weight Cutoff (Spectrum Laboratories) and dialyzed at 4 °C against water. Following dialysis, the sample centrifuged for 3 h at 100,000 × *g*. The supernatant was discarded, and the pellet was resuspended in 1 mL of deionized water by trituration (one-fifth of the original homogenate volume).

sPMCA. For experiments comparing cofactor PrP^{Sc} with protein-only PrP^{Sc} molecules, reconstituted sPMCA reactions were conducted as previously reported (20), with the following modifications. Sonication pulses were 15 s every 30 min with power output ~215 W, and 100 μL reactions contained 6 μg /mL recombinant mouse PrP (MoPrP), 20 mM Tris (pH 7.5), 135 mM NaCl, 5 mM EDTA (pH 7.5), 0.15% (vol/vol) Triton X-100 supplemented with either cofactor or water as indicated. The original $recPrP^{Sc}$ seed used for these experiments was generated de novo by F.W. as previously described (22) and then was propagated by sPMCA with recPrP and purified cofactor by N.R.D. Cofactor PrP^{Sc} and protein-only PrP^{Sc} samples were propagated by sPMCA (18 rounds) using the same $recPrP^{Sc}$ seed and base substrate mixture (with the addition of either cofactor for cofactor PrP^{Sc} samples or water for protein-only PrP^{Sc} samples, as indicated) and were processed in parallel in concentric positions relative to the center of the same microplate horn.

For experiments comparing different prion strains as seed, 100-μL reactions contained 6 μg /mL recombinant MoPrP, 20 mM Tris (pH 7.5), 135 mM NaCl, 5 mM EDTA (pH 7.5), 0.15% (vol/vol) Triton X-100, and either 25 μL purified cofactor or 10 mM plasmalogen PE [resuspended in 0.05% (vol/vol) Triton X-100]. Day 1 reactions were seeded with 10 μL of scrapie brain homogenate diluted 1:10 in PBS or with 10 μL $recPrP^{Sc}$. Samples were sonicated with 15-s pulses every 30 min for 24 h at 37 °C. After each 24-h period, 1/10th of the reaction volume was transferred to a different tube containing fresh substrate mixture, and the 24-h cycle of sonication was repeated. To prevent cross-contamination between samples, all tubes were sealed with Parafilm (Pechiney Plastic Packaging Company) and clamped shut using a plastic holder (30). Separate strains were propagated at different times in separate sonicator horns (either new or presoaked in 100% bleach) to avoid the possibility of cross-contamination between strains. Each sample was propagated for 18 rounds to eliminate the original seed by serial dilution. The effectiveness of this dilution was confirmed for each sample by performing mock propagation reactions of seeded samples lacking PrP substrate for 18 rounds. The lack of infectivity in these mock-propagated samples confirmed the adequacy of serial dilution to eliminate the original seed as well as our ability to prevent cross-contamination. To confirm that our substrate materials and inocula were not contaminated, we inoculated unseeded substrate mixture that was not subjected to sPMCA.

Seeded sPMCA experiments using normal mouse brain homogenate as substrate were performed as previously described (33).

PrP^{Sc} Detection. To detect PrP^{Sc} molecules in either the products of PMCA reactions or brain homogenates (5% wt/vol in PBS 0.5% (vol/vol) Triton X-100), samples were digested with 25 μg/mL proteinase K for 30 min at 37 °C. All samples were processed for SDS/PAGE and Western blotting as previously described (29), substituting Towbin transfer buffer (34) and using mAb 6D11 as the primary antibody. SDS/PAGE signals were quantified using Image Gauge v4.22 (Fujifilm). PrP levels were determined semiquantitatively by comparison with a dilution series of recPrP as standard.

Scrapie Inoculation and Diagnosis. Samples containing PMCA products were prepared and serially diluted in sterile PBS 1% (wt/vol) BSA. PMCA samples were diluted directly 1:10 (i.e., without prior concentration) to generate the 10^{-1} titer sample. Samples of brain homogenates were adjusted to 1% (wt/vol) final concentration in PBS 1% (wt/vol) BSA for inoculation. Intracerebral inoculations (using a volume of 30 μL) and scrapie diagnosis in C57BL female mice were performed as described previously (20).

Neuropathology. Mice were killed, and brains were removed rapidly using new, sterile-packaged dissection instruments and disposable surfaces to avoid cross-contamination. Brains were immersion-fixed in 10% (wt/vol) buffered formalin for 2–30 d, cut into ~3-mm-thick sagittal sections, and placed in a tissue-processing cassette. Cassettes were treated with 88% formic acid for 1 h and then were stored in PBS. The tissue was processed for paraffin embedding, and representative slides were stained with H&E. Immunohistochemistry was performed on deparaffinized slides using 2 μg/mL 27/33 anti-PrP mAb for 30 min at room temperature after citrate antigen retrieval and a Biocare Mouse on Mouse development kit. Blinded scoring for vacuolation and PrP deposition was performed using standard scales as described previously (20).

Atomic Force Microscopy. PMCA reactions were pooled to a total volume of 1,250 μL. Each tube received 100 μL of a 50% (vol/vol) slurry of immobilized L-1-tosylamido-2-phenylethyl chloromethyl ketone (TPCK)-treated trypsin (catalog no. 20230; Thermo Scientific) and was incubated overnight at 37 °C while rotating end over end. The next morning each tube was centrifuged briefly to pellet the agarose beads. After the supernatant was removed, each tube was centrifuged at 100,000 × *g* for 1 h. A 250-μL pellet was resuspended to 1,200 μL in 3% (wt/vol) NOG and then was centrifuged at 100,000 × *g* for 1 h. Again, a 250-μL pellet was washed with 3% (wt/vol) NOG followed by two washes in 1 mL of water. The final pellet was vortexed for 20 s, sonicated for 20 s at power 65, and vortexed again for 20 s. A small amount then was treated with 25 μg/mL of proteinase K, and the concentration was determined by Western blot and densitometry.

Samples were scanned by atomic force microscopy as previously described (33). Briefly, images were captured in tapping mode using two different tips [TAP300AL cantilever with a tip radius <10 nm and a force constant of 40 N/m (Budget Sensors) or SSS-NCHR cantilever with a tip radius <2 nm and a force constant of 42 N/m (Nanosensors)]. Each sample (15 μL) was laid down on a piece of freshly cleaved mica and allowed to dry under nitrogen. Samples were rinsed three times with 150 μL of water. Data were collected as 512 × 512 pixel images, using multiple samples and several scanning sessions. Images were exported using Gwyddion 2.19 software (Czech Metrology Institute).

Fluorescence Double-Color Assay. Two hundred microliters of $recPrP^{Sc}$ [prepared by three rounds sPMCA using 0.5 mM NBD-PE (Avanti Polar Lipids) as a cofactor] was adjusted to 1.5-mL total volume with PBS 1% (vol/vol) Triton, centrifuged at 100,000 × *g* for 1 h, and washed three times with PBS 3% (wt/vol) NOG and once with PBS. The pellet was resuspended in 100 μL 10 mM acetate buffer, pH 5.0, and incubated for 1 h at room temperature and then overnight at 4 °C in a Permanox eight-well Lab-Teks chamber slide system (Nunc) in 10 mM sodium acetate, pH 5.0. The following day, the samples were fixed to the slide by the addition of 150 μL of PBS, 8% (vol/vol) formaldehyde and incubation at room temperature for 15 min. Unfixed sample was removed by aspiration, and each slide well was washed once with 150 μL of PBS. Then 150 μL of mAb D13 diluted 1:250 in PBS + 4% (wt/vol) BSA was applied to each slide well and allowed to incubate overnight at 4 °C or for 2 h at room temperature in a humidified chamber. After primary antibody incubation, the slide well was washed three times with 150 μL of PBS + 4% (wt/vol) BSA and was allowed to incubate for 15 min at room temperature during each wash. Then150 μL of secondary antibody, sheep anti-mouse conjugated with Alexa Fluor 568 (Invitrogen), diluted 1:250 in PBS + 4% (wt/vol) BSA, was applied to each slide and allowed to incubate for 2 h in the dark at room temperature in a humidified chamber. The slide well then was washed three times with 150 μL of PBS + 4% (wt/vol) BSA and was allowed to incubate for 15 min at room temperature during each wash. ProLong Antifade

solution (15 μL) (Invitrogen) was added to each sample and 18-mm^2 glass coverslips (catalog no. 1.5; Corning) were mounted on each slide and allowed to dry overnight in the dark in a desiccating chamber. We also prepared and analyzed a control slide coated with reaction buffer only and then stained with D13 mAb and Alexa Fluor 568 secondary antibody to rule out nonspecific binding of either antibody to the slide. A slide coated only with NBD-PE in reaction buffer was prepared to rule out nonspecific binding of NBD-PE to the slide. Finally, a slide coated with PrP^{Sc} in reaction buffer that did not contain NBD-PE was prepared to rule out autofluorescence of PrP^{Sc} in the NBD excitation wavelength. Samples were analyzed visually using a Zeiss Axioplan 2 wide-field fluorescence microscope, and digital images were captured with Phylum Live 4.2.1 software (Improvision).

Statistical Methods. We used nonparametric approaches to compare the vacuolation characteristics in seven brain regions and immunohistochemical (IHC) deposition in eight brain regions of animals inoculated with OSU input (n = 5), Me7 input (n = 6), 301C input (n = 5), OSU cofactor (n = 6), Me7 cofactor (n = 8), 301 cofactor (n = 8), OSU PE (n = 7), Me7 PE (n = 5), or 301C PE (n = 7). Specifically, we used Mann–Whitney tests to compare IHC characteristics in each brain region from each input strain (OSU, Me7, and 301C) with its corresponding cofactor strain. We used Kruskal–Wallis equality-of-populations rank tests to assess the probability that the IHC characteristics seen within each brain region for the six output strains represented a single distribution. We repeated the analysis including all nine strains to test the hypothesis that the IHC patterns for all nine strains represent a single distribution. We defined $P < 0.05$ as statistically significant. Data were analyzed using Stata 12.0 (Stata Corporation).

Enzymatic Deglycosylation. Various 10% brain homogenates were normalized for PrP scrapie content by dilution in $PrnP^{0/0}$ brain homogenate. Seventy-five microliters of each homogenate was added to 25 μL of PBS, 2% (vol/vol) Triton X-100 containing 40 μg/mL proteinase K, and samples were shaken at 750 rpm for 30 min at 37 °C. After incubation, 5 μL of 200 mM PMSF (in 100% EtOH) was added, and the sample was vortexed and incubated at room temperature for 10 min. Next, samples were diluted with 895 μL PBS, 0.5% (vol/vol) Triton X-100 and were centrifuged at 100,000 × g for 60 min at 4 °C, and supernatants were discarded. Pellets then were resuspended in 20 μL of 5× glycoprotein denaturation buffer, subjected to three 30-s bursts of sonication, and boiled at 95 °C for 10 min. Samples then were diluted with 80 μL water, and sonication and boiling were repeated. Next, samples were cooled to room temperature, and 13 μL each of 10× G7 reaction buffer and 10% (vol/vol) Nonidet P-40 and 5 μL of peptide:N-glycosidase F (PNGase F) were added to each sample. Samples were incubated overnight at 37 °C. Reactions were stopped by the addition of 44 μL of 4× SDS sample buffer and boiling at 95 °C for 10 min.

Urea Denaturation Assay. Thirty microliters of 10% (wt/vol) brain homogenate was mixed with 120 μL of various urea/0.25% (vol/vol) Triton X-100 solutions to obtain final urea concentrations between 0 and 8 M. Samples then were incubated at 60 °C for 3 h with shaking at 750 rpm. Next, 100 μL of 50 mM Mops (pH 7.0) containing 330 mM NaCl, 1% (vol/vol) Triton X-100, and 125 μg/mL proteinase K was added, and samples were incubated at 37 °C for 45–60 min, with shaking at 750 rpm. Then 84 μL of 4× SDS sample buffer was added, and samples were boiled for 10 min at 95 °C. SDS/PAGE signals were quantified using Image Gauge v4.22 (Fujifilm).

ACKNOWLEDGMENTS. We thank Dr. Charles Daghlian for helpful advice on atomic force microscopy protocols, Drs. Charles Daghlian and Ekaterina Pletneva for helpful advice on Raman spectroscopy protocols, and Ann Lavanway for help with fluorescence microscopy. Financial support for this study was provided by National Institutes of Health Grants 2R01 NS046478, R01 NS055875, R01 NS071035, and R01 NS060729.

1. Prusiner SB (1982) Novel proteinaceous infectious particles cause scrapie. *Science* 216: 136–144.
2. Caughey BW, et al. (1991) Secondary structure analysis of the scrapie-associated protein PrP 27-30 in water by infrared spectroscopy. *Biochemistry* 30:7672–7680.
3. Pan KM, et al. (1993) Conversion of alpha-helices into beta-sheets features in the formation of the scrapie prion proteins. *Proc Natl Acad Sci USA* 90:10962–10966.
4. Kocisko DA, et al. (1994) Cell-free formation of protease-resistant prion protein. *Nature* 370:471–474.
5. Deleault NR, Harris BT, Rees JR, Supattapone S (2007) Formation of native prions from minimal components in vitro. *Proc Natl Acad Sci USA* 104:9741–9746.
6. Griffith JS (1967) Self-replication and scrapie. *Nature* 215:1043–1044.
7. Supattapone S (2010) Biochemistry. What makes a prion infectious? *Science* 327: 1091–1092.
8. Surewicz WK, Apostol MI (2011) Prion protein and its conformational conversion: A structural perspective. *Top Curr Chem* 305:135–167.
9. Colby DW, Prusiner SB (2011) De novo generation of prion strains. *Nat Rev Microbiol* 9:771–777.
10. Colby DW, et al. (2010) Protease-sensitive synthetic prions. *PLoS Pathog* 6:e1000736.
11. Makarava N, et al. (2010) Recombinant prion protein induces a new transmissible prion disease in wild-type animals. *Acta Neuropathol* 119:177–187.
12. Kim JI, et al. (2010) Mammalian prions generated from bacterially expressed prion protein in the absence of any mammalian cofactors. *J Biol Chem* 285:14083–14087.
13. Bosque PJ, Prusiner SB (2000) Cultured cell sublines highly susceptible to prion infection. *J Virol* 74:4377–4386.
14. Klöhn PC, Stoltze L, Flechsig E, Enari M, Weissmann C (2003) A quantitative, highly sensitive cell-based infectivity assay for mouse scrapie prions. *Proc Natl Acad Sci USA* 100:11666–11671.
15. Piro JR, Harris BT, Supattapone S (2011) In situ photodegradation of incorporated polyanion does not alter prion infectivity. *PLoS Pathog* 7:e1002001.
16. Bruce ME (1993) Scrapie strain variation and mutation. *Br Med Bull* 49:822–838.
17. Carlson GA (1996) Prion strains. *Curr Top Microbiol Immunol* 207:35–47.
18. Angers RC, et al. (2010) Prion strain mutation determined by prion protein conformational compatibility and primary structure. *Science* 328:1154–1158.
19. Li J, Browning S, Mahal SP, Oelschlegel AM, Weissmann C (2010) Darwinian evolution of prions in cell culture. *Science* 327:869–872.
20. Deleault NR, Kascsak R, Geoghegan JC, Supattapone S (2010) Species-dependent differences in cofactor utilization for formation of the protease-resistant prion protein in vitro. *Biochemistry* 49:3928–3934.
21. Deleault NR, et al. (2012) Isolation of phosphatidylethanolamine as a solitary cofactor for prion formation in the absence of nucleic acids. *Proc Natl Acad Sci USA* 109: 8546–8551.
22. Wang F, Wang X, Yuan CG, Ma J (2010) Generating a prion with bacterially expressed recombinant prion protein. *Science* 327:1132–1135.
23. Atarashi R, et al. (2007) Ultrasensitive detection of scrapie prion protein using seeded conversion of recombinant prion protein. *Nat Methods* 4:645–650.
24. Mathur V, Taneja V, Sun Y, Liebman SW (2010) Analyzing the birth and propagation of two distinct prions, [PSI+] and [Het-s](y), in yeast. *Mol Biol Cell* 21:1449–1461.
25. Tyedmers J, et al. (2010) Prion induction involves an ancient system for the sequestration of aggregated proteins and heritable changes in prion fragmentation. *Proc Natl Acad Sci USA* 107:8633–8638.
26. Castilla J, et al. (2008) Cell-free propagation of prion strains. *EMBO J* 27:2557–2566.
27. Colby DW, et al. (2009) Design and construction of diverse mammalian prion strains. *Proc Natl Acad Sci USA* 106:20417–20422.
28. Legname G, et al. (2005) Strain-specified characteristics of mouse synthetic prions. *Proc Natl Acad Sci USA* 102:2168–2173.
29. Piro JR, et al. (2009) Prion protein glycosylation is not required for strain-specific neurotropism. *J Virol* 83:5321–5328.
30. Cosseddu GM, et al. (2011) Ultra-efficient PrP(Sc) amplification highlights potentialities and pitfalls of PMCA technology. *PLoS Pathog* 7:e1002370.
31. Collinge J, Clarke AR (2007) A general model of prion strains and their pathogenicity. *Science* 318:930–936.
32. Jucker M, Walker LC (2011) Pathogenic protein seeding in Alzheimer disease and other neurodegenerative disorders. *Ann Neurol* 70:532–540.
33. Piro JR, et al. (2011) Seeding specificity and ultrastructural characteristics of infectious recombinant prions. *Biochemistry* 50:7111–7116.
34. Towbin H, Staehelin T, Gordon J (1979) Electrophoretic transfer of proteins from polyacrylamide gels to nitrocellulose sheets: Procedure and some applications. *Proc Natl Acad Sci USA* 76:4350–4354.
35. Nishina KA, et al. (2006) The stoichiometry of host PrPC glycoforms modulates the efficiency of PrPSc formation in vitro. *Biochemistry* 45:14129–14139.
36. Baskakov IV, Legname G, Baldwin MA, Prusiner SB, Cohen FE (2002) Pathway complexity of prion protein assembly into amyloid. *J Biol Chem* 277:21140–21148.